BALANCING THE VOLTAGE OF A THREE-PHASE FLYING CAPACITOR CONVERTER BY SUPPLYING AN INDUCTION MOTOR

D SRINIVAS[*] , Dr. B.V.Sanker Ram[**] ,A Lakshmisudha[***]

[*]Pursuing Ph.D   in power electronics from to JNTUK

[**]Professor,jntuh, B.E. (Electrical) O. U, M.Tech. (PS) O.U, Ph.D, JNTU.

[***]Post Graduate student ,pragati engg college,Kakinada,ap,india

Abstract - The natural voltage balancing the dynamics of a three-phase flying capacitor converter when supplying an induction motor is analyzed in this paper. Double fourier harmonic series is used for the pulse width modulation switching waveforms and the frequency response of the motor, to create a linear state-space model of this type of load. The mid-frequency response (500 Hz–20 kHz) of the induction motor impedance is identified, and skin and proximity effects are considered by adding parallel R–L networks to a standard motor model. FFT analysis is applied to variable frequency square waves which were injected into the motor terminals to measure the model parameters and least squares minimization method is used to find fitting parameter values to these measurements. As a result the converter voltage balancing behavior degrades considerably at low motor speeds, and that a balance booster filter, as formerly proposed, significantly improves the dynamic response. A scaled-down flying capacitor converter drive is used for experimental confirmation.

Key words- Capacitor, Motor Drive, Flying Capacitor, Induction.

I. INTRODUCTION

The Increasing demand for high-power variable-speed drives at medium voltages has been a major technology driver for the multilevel power converter market [1], [2]. The attraction of these converters is that they elegantly overcome the intrinsic voltage limits of semiconductor switches, by combining series strings of devices with a network of passive storage elements to constrain device-operating voltages. They also allow the synthesis of stair-case envelope-switched waveforms that achieve reduced harmonic distortion [1] and common-mode voltages [3], compared to conventional two-level structures. Three major multilevel converter structures exist: the diodeclamped,cascaded, and flying capacitor topologies [1], [2]. The diode-clamped topology uses a series capacitor string to subdivide a single high-voltage dc link into the required number of voltage levels. A network of clamping diodes then limits each device's voltage as the phase legs switch between the intermediate voltage levels [1]. This topology has the advantage of transformerless operation, but control of the capacitor voltages remains a challenging problem [1]. In contrast, a cascaded converter uses series connected H-bridge modules, each energized from separate galvanically isolated dc supplies [1], [3].
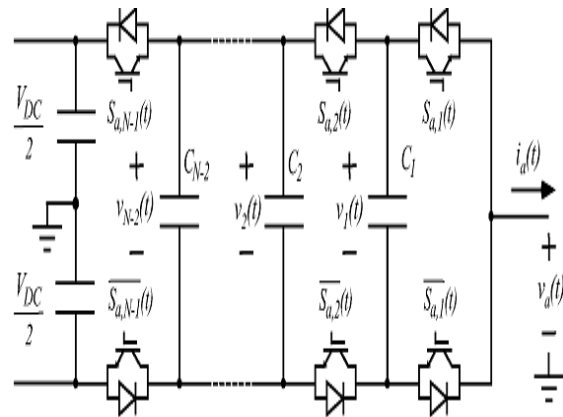

Fig1: Structure of an N-level flying capacitor phase leg (phase a).

This solves the intermediate voltage regulation problem, but the supplies are typically derived from a low-frequency transformer or high-frequency dc–dc converter, which adds cost, weight, and volume to the final system [1].
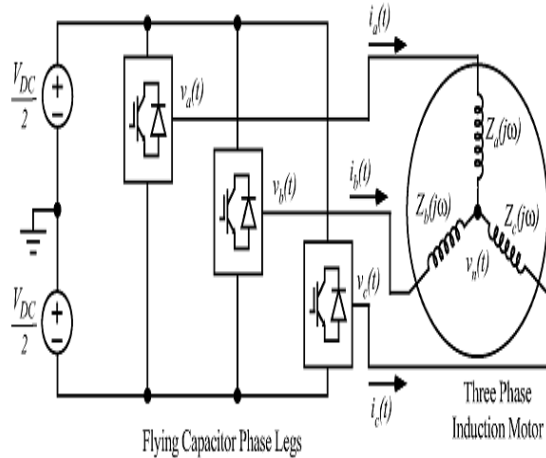
Fig.2: Overall three-phase flying capacitor converter.

One promising capacitor voltage control method is natural balancing [5]–[9], which requires modulation strategies that maintain the cell duty cycles at approximately equal values. This is most easily achieved using phase-shifted carrier pulsewidth modulation (PSCPWM) [9], [10], illustrated in Fig. 2. Recent work has also demonstrated that the harmonically optimal One promising capacitor voltage control method is natural balancing [5]–[9], which requires modulation strategies that maintain the cell duty cycles at approximately equal values. This is most easily achieved using phase-shifted carrier pulsewidth modulation (PSCPWM) [9], [10], illustrated in Fig. 3.
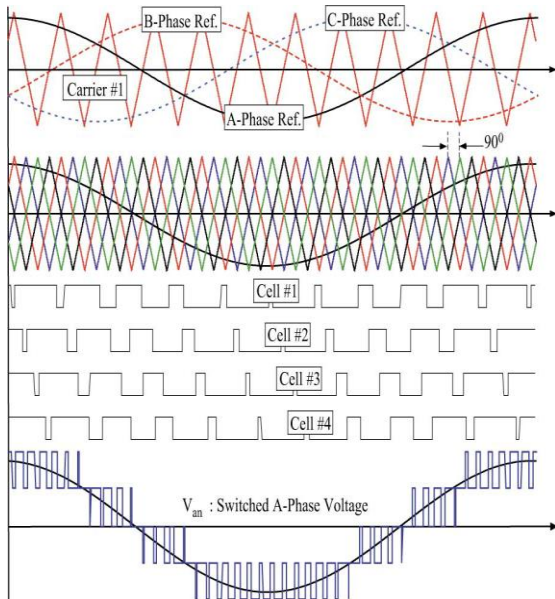

Fig .3: Phase-shifted carrier (PSC) PWMapplied to a five-level flying capacitor converter, showing the

resultingA-phase cell command signals and switched A-phase voltage.

Recent work has also demonstrated that the harmonically optimal phase disposition and centered space vector PWM methods can achieve similar results [1]. However, while natural balancing has been studied at length, most of the work has considered only resistive–inductive loads, due to the complexity of the nonlinear analysis process.

II BALANCE MODELS

If the load current is smooth, and the cells are switched with interleaved waveforms of equal duty cycles (see Fig. 3), it can be readily shown that the average floating capacitor currents will be zero, with no associated capacitor voltage drift [5]. However, this analysis fails to explain why the capacitor voltages will naturally evolve to their target operating points under the same switching behavior.

A. Capacitor Voltage Balance Model:

In [7]–[9], it was shown that while the transient circuit equations for the flying capacitor converter are nonlinear, this complexity can be eliminated using a double Fourier series representation of the converter switching waveforms. This eliminates the load current terms from the converter dynamic equations, yielding a linear state-space equation with the capacitor voltages as the system states, and the dc link voltage as the system input, viz.

$$\dot{\mathbf{V}}_{\mathbf{c}}(t) = \mathbf{A}\mathbf{V}_{\mathbf{c}}(t) + \mathbf{B}V_{\mathrm{DC}} \qquad (1)$$

where the capacitor voltage matrix is given by

$$\mathbf{V}_{\mathbf{c}}(t) = \begin{bmatrix} \mathbf{V}_{ca}(t) & \mathbf{V}_{cb}(t) & \mathbf{V}_{cc}(t) \end{bmatrix}^{T} \qquad (2)$$

$$\mathbf{V}_{\mathbf{ca}}(t) = \begin{bmatrix} v_{a,1}(t) & \dots & v_{a,N-2}(t) \end{bmatrix}^{T} \qquad (3)$$

$$\mathbf{V}_{\mathbf{cb}}(t) = \begin{bmatrix} v_{b,1}(t) & \dots & v_{b,N-2}(t) \end{bmatrix}^{T} \qquad (4)$$

$$\mathbf{V}_{\mathbf{cc}}(t) = \begin{bmatrix} v_{c,1}(t) & \dots & v_{c,N-2}(t) \end{bmatrix}^{T} \qquad (5)$$

and the A and B state-space matrices are defined by the modulation and load conditions. The coefficients of A and B are derived as follows: The harmonic representation of the switched waveform Sx,k (t) produced by a sine-triangle PWM process is best defined by a double Fourier series, given by [10]

$$S_{x,k}(t) = \frac{C_{00}}{2} + \sum_{n=1}^{\infty} [C_{0n} \cos(n[\omega_o t + \phi_x])]$$

$$+ \sum_{m=1}^{\infty} \sum_{n=-\infty}^{\infty} \left[C_{mn} \cos \begin{pmatrix} m[\omega_c t + \phi_{c,k}] \\ +n[\omega_o t + \phi_x] \end{pmatrix} \right] \quad (6)$$

terms defined are small in the vicinity of the dominant switching harmonics. This concept has led a number of researchers [2], [5], [7] to propose the use of balance booster filter networks (i.e., tuned series R–L–C networks in parallel to the load).
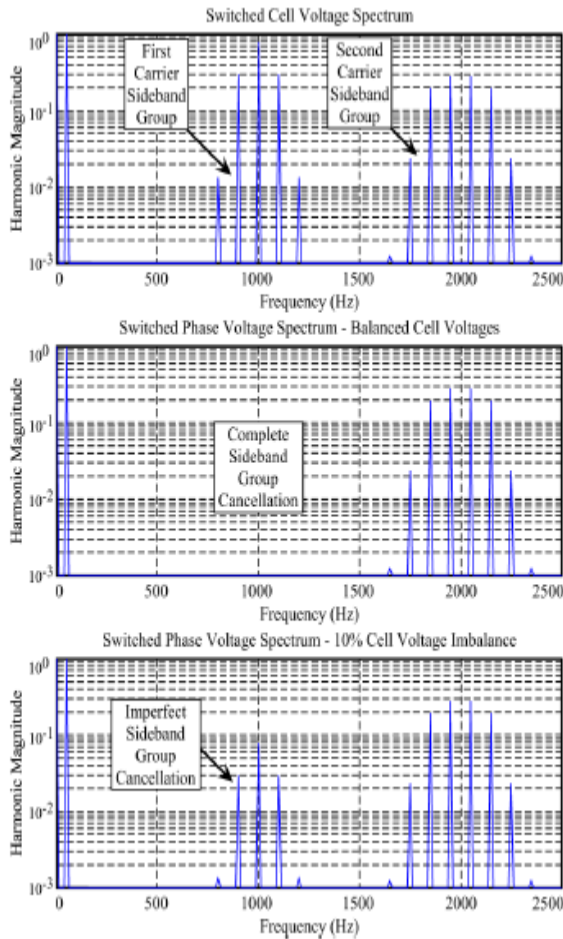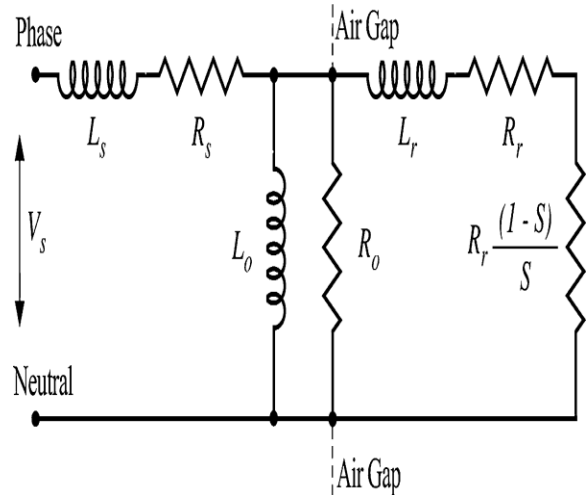

Fig.4: Cell and phase voltage spectra for PSCPWM, considering balanced and unbalanced conditions. M = 0.9, fc = 1000 Hz, fo = 50 Hz.

B. Balance Booster Filters:

The dependence of the balancing response on the load impedance can be inferred, since the balancing time constants are the inverse of the system poles (i.e., eigenvalues of the A matrix), according to

$\tau k = -1/\lambda k$, where det $[\lambda k \; \mathbf{I} - \mathbf{A}] = 0$. (7)

If the noninteractive terms dominate the A-matrix, then for large diagonal entries, the resulting time constants will be relatively short lived. This requires that the load impedance

Fig.5: Per-phase steady-state induction motor model.
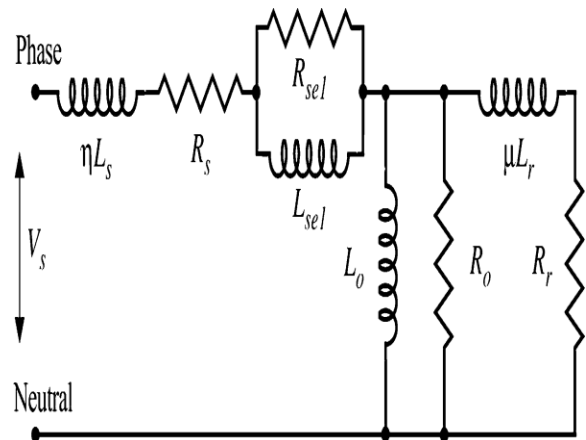

Fig.6: Per-phase mid-frequency band induction motor model.

III. SYSTEM MODEL

To apply the voltage balance model to a drive scenario, the frequency response of the induction motor must be obtained throughout the frequency range of the significant switching harmonics. For medium-voltage drives, carrier frequencies are generally in the range of 1–2 kHz for IGBT's [1], [4]. Hence, for ten sideband groups, as required in the balance model, the frequency range of interest extends from 500 Hz to 20 kHz, corresponding to the mid-frequency band for an induction motor [3].

Three major model refinements are made to account for midfrequency behavior. First, since the harmonic excitation frequencies are normally at least a factor of 10 larger than the fundamental frequency, the machine slip is set to unity, eliminating the virtual resistor from the motor model. This is a significant simplification, as it shows that the machine mid-frequency behavior is independent of the mechanical load (as is also consequently true for the converter capacitor voltage balancing dynamics). The second refinement concerns skin and proximity effects in the machine windings, which become significant at midfrequencies [2], [15]. A standard way to account for these effects is to include parallel R–L networks in series with the machine stator windings [2], as illustrated in the mid-frequency model of Fig. 5. While higher order networks have been reported [2], recent work indicates that a first-order network is generally sufficient [3], [5].

Motor Parameters			Value
Stator Winding Resistance	(R_s)	(Ω)	2.16
Stator Leakage Inductance	(L_s)	(mH)	15.5
Rotor Winding Resistance	(R_r)	(Ω)	2.74
Rotor Leakage Inductance	(L_r)	(mH)	15.5
Core Loss Resistance	(R_0)	(Ω)	426
Magnetising Inductance	(L_0)	(mH)	451

Table.1: Measured Steady-State Induction Motor Parameters
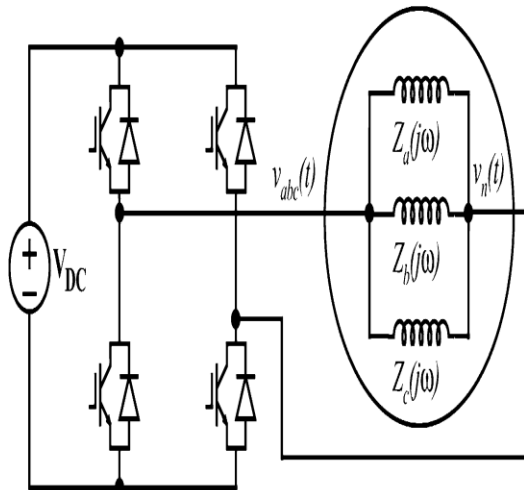

Fig. 7. Induction Motor Characterization Test Circuit.

The third refinement is to recognize that the motor leakage inductance depends on the applied excitation frequency [3].Since the

balancing model does not depend on the low-frequency properties of the induction motor, this variation can be represented by an average scaling of the motor low-frequency stator and rotor leakage terms Ls and Lr by the parameters η and μ. However, to apply the resulting per-phase motor circuit to the natural balancing model, characterization tests must be carried out throughout the mid-frequency band.

IV. ANALYTIC VOLTAGE BALANCE RESPONSE

A three-level three-phase converter with the circuit parameters identified was investigated, loaded by the deltaconnected induction motor. (Note that since the balance model assumes a wye-connected load impedance, the motor Thevenin equivalent impedance was determined using a wye-delta impedance transformation.) Aconstant volts/hertz functionwas applied, with themodulation index and fundamental frequency defined according to

Circuit Parameter		Value
Nominal DC Link Voltage	(V_{DC})	250 V
Flying Capacitors	(C_k)	30 µF
Carrier Frequency	(f_c)	2100 Hz
Balance Booster Inductance	(L_B)	500µH
Balance Booster Capacitance	(C_B)	12 µF

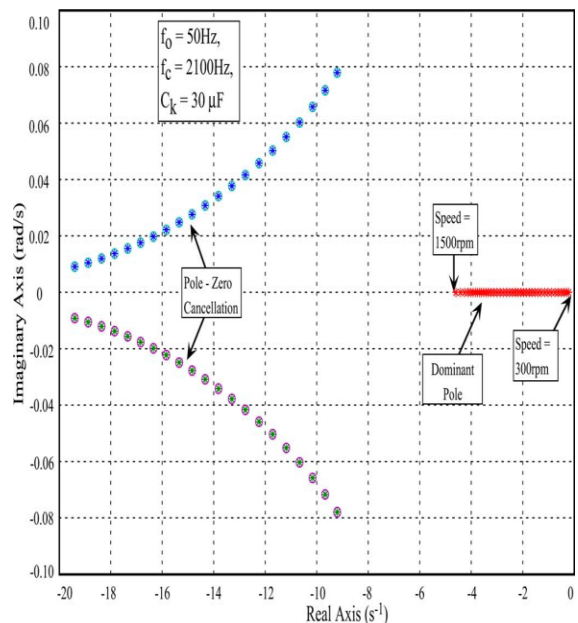Table.2: Three-Level Converter—Circuit Parameters

Fig.8: Root locus of the three-level converter as a function of motor speed no balance booster connected.
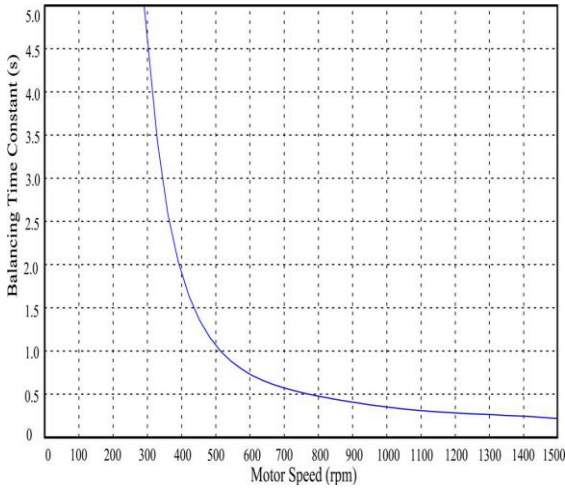

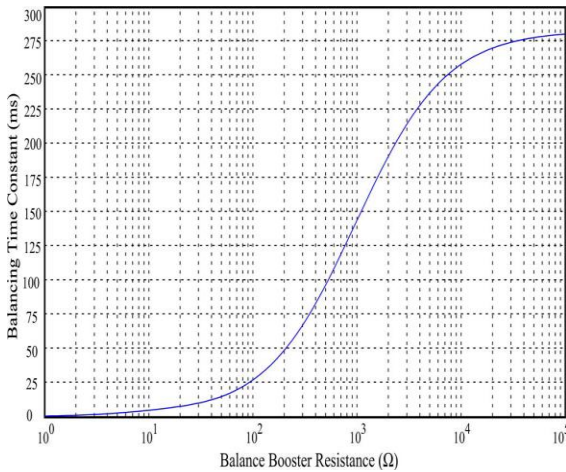Fig.9: Balancing time constant as a function of motor speed—no balance booster connected.

Fig.10: Balancing time constant as a function of the balance booster resistance *RB* —motor speed = 1200 r/min, *M* = 0.8, fo = 40 Hz.
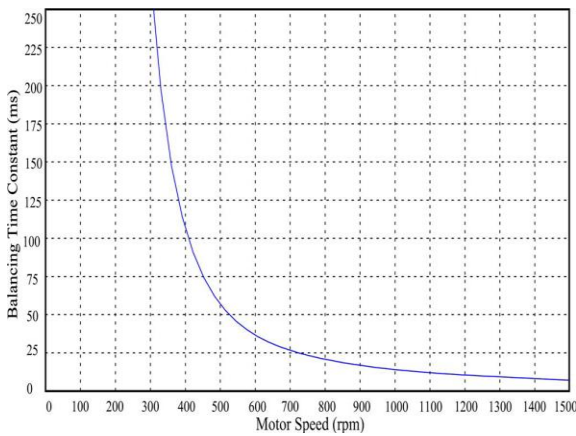

Fig.11: Fig. 11. Balancing time constant as a function of motor speed—balance booster connected with *RB* = 20 Ω.

Showing the dominant time constant as a function of speed. These results show that the balancing behavior degrades at low speeds, largely due to the modulation index reduction. This response is likely to be unacceptable for most practical drive systems.

V. RESULTS

The balancing dynamics of the flying capacitor drive were investigated by comparing the analytic model predictions against a low-voltage flying capacitor converter, with the parameters given in Table II. The experimental converter was controlled using PSCPWM, implemented using three TMSC240DSP controllers. Each DSP generated the gate signals for one three-level phase leg, using a carrier and reference waveform synchronization strategy similar to that reported in [3]. Since the converter ratings are limited to a 250 V dc link, the induction motor was connected in delta, with a parallel wye-connected balance booster filter. A constant volts/hertz modulation profile was used, and link voltage transient events were introduced via a controllable dc source. ig. 14 shows the experimental converter waveforms for a steady-state operating condition. The three voltage levels in the switched phase leg voltage are clearly evident, confirming that
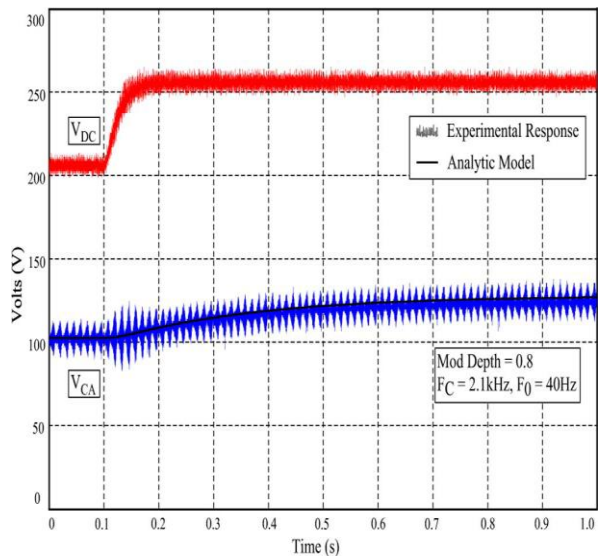

Fig.12: Comparison of experimental and analytic transient response of the three-level drive to a dc link step. No balance booster.
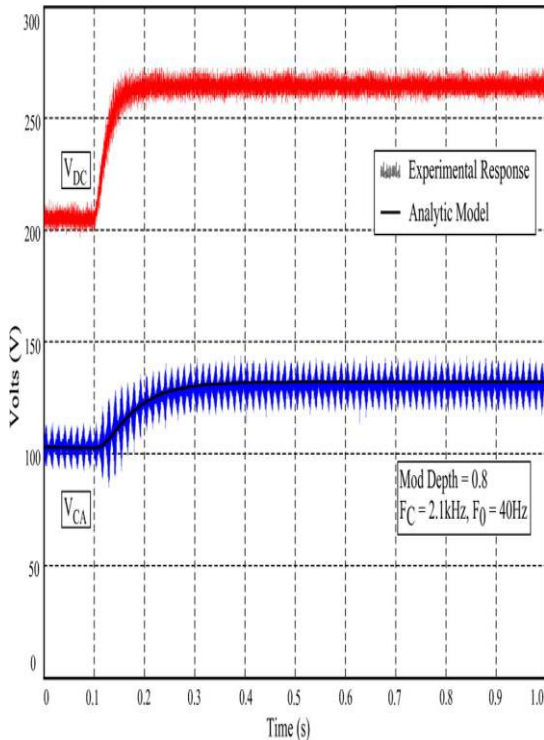
Fig.13: Comparison of experimental and analytic transient response of the three-level drive to a dc link step. Balance booster with $RB = 300 \ \Omega$.
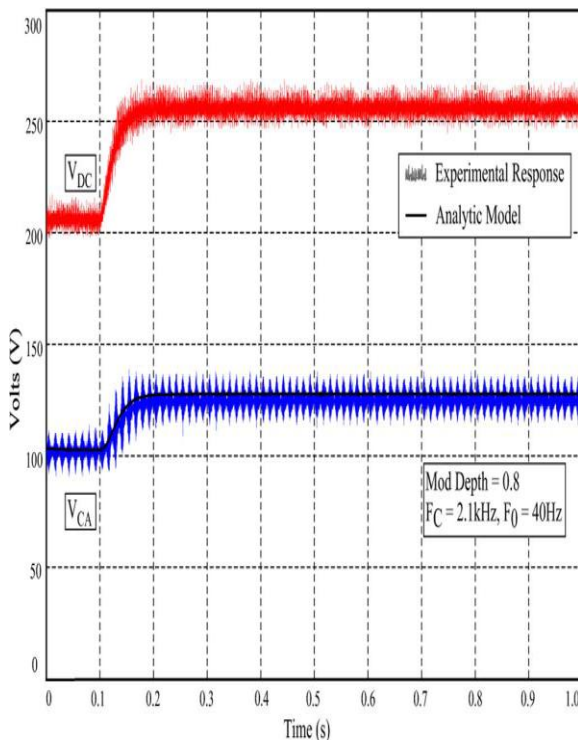

Fig14: Comparison of experimental and analytic transient response of the three-level drive to a dc link step. Balance booster with $RB = 20 \ \Omega$.

Natural balance has been achieved, and verifying the experimental implementation. Fig. 15 shows the experimental and analytic transient balancing response of the flying capacitor converter for a dc link step change with the balance booster isolated. The natural balancing behavior is clearly evident, as the capacitor voltage drives to 50% of the new link voltage condition. The analytic response, computed in MATLAB, shows excellent agreement with the experimental trace, validating the mid-frequency induction motor model.

CONCLUSION

The natural capacitor voltage balancing dynamics of a three phase flying capacitor converter supplying an induction motor load is determined using the proposed analytical method. This investigative technique make a whole of the previously developed balance models with a mid-frequency (500 Hz–20 kHz) induction motor model that accounts for skin and proximity effects in the motor windings. The motor impedance is determined via high frequency square wave injection using the presented categorization method and least-squares minimization is used to fit the motor model according to the data. The converter balancing dynamics were explored over a wide range of conditions using the resulting logical model. The results show the balancing dynamic degrades at a sharper rate in the low-speed region of operation with a small modulation index. The converter balancing response is improved by exploring the design of a balance booster filter. These filters help in a time constant improvement of an order of magnitude. . This investigative process facilitates the design of these filters, including the calculation of the additional rms current loading that the balance booster introduces to the converter. Finally the diagnostic results have been tested against experimental results obtained using a low voltage flying capacitor converter.

REFERENCES

[1] D. G. Holmes and T. A. Lipo, Pulse Width Modulation for Power Converters. Piscataway, NJ: IEEE Press, 2003.

[2] B. P. McGrath, G. Gateau, T. Meynard, and D. G. Holmes, "Optimal modulation of flying capacitor and stacked multicell converters using a state machine decoder," IEEE Trans. Power Electron., vol. 22, no. 2,pp. 508–516, Mar. 2007.

[3] R. J. Gorter, A. Veltman, and P. van den Bosch, "Skin effect impact on induction motor parameters

estimation using an output-error identification method," in Proc. IEEE Power Electron. Spec. Conf. (PESC), 1994,pp. 763–768

[4] P. C. Loh, D. G. Holmes, and T. A. Lipo, "Implementation and control of distributed PWM cascaded multilevel inverters with minimal harmonic distortion and common mode voltage," IEEE Trans. Power Electron., vol. 20, no. 1, pp. 90–99, Jan. 2005.

[5] D. Krug, S. Bernet, S. Saeed Fazel, K. Jalili, and M. Malinowski, "Comparison of 2.3 kV medium-voltage multilevel converters for industrial medium-voltage drives," IEEE Trans. Ind. Electron., vol. 54, no. 6, pp. 2979–2992, Dec. 2007.

[6] R. Wilkinson, H. du Mouton, and T. Meynard, "Natural balance of multicell converters: The general case," IEEE Trans. Power Electron., vol. 21, no. 6, pp. 1658–1666, Nov. 2006.

[7] B. McGrath and D. G. Holmes, "Analytical modelling of voltage balance dynamics for a flying capacitor multilevel converter," IEEE Trans. Power Electron., vol. 23, no. 2, pp. 543–550, Mar. 2008.

[8] J. Rodriguez, S. Bernet, B.Wu, J. Pontt, and S.Kouro, "Multilevel voltagesource- converter topologies for industrial medium-voltage drives," IEEE Trans. Ind. Electron., vol. 54, no. 6, pp. 2930–2945, Dec. 2007.

[9] T.Meynard,H. Foch, P. Thomas, J. Courault, R. Jakob, andM.Nahrstaedt, "Multicell converters: Basic concepts and industry applications," IEEE Trans. Ind. Electron., vol. 49, no. 5, pp. 955–964, Jun. 2002.

Author's List

D SRINIVAS received B.Tech,M.Tech in EEE from JNTUH, Pursuing Ph.D in power electronics from to JNTUK. He is a live student Member of IEEE & IEEE electrical Society. His research areas of interest are power electronics & electrical machines.

Dr.B.V.Sanker Ram, Professor,jntuh, B.E. (Electrical) O.U, M.Tech.(PS)O.U, Ph.D,JNTU. Published more than 20 Research papers in International Journals, morethan 30 papers in International and National Conference, Guding 15 Ph.D. Candidates.Areas Of Interest Power Electrics, Power System, FACTS, PQ.

A Lakshmisudha ,Completed her b.Tech from JNTU. Presently persuing M.Tech from Pragati engg college,Kakinada,ap,india.Her area of interest are power electronics & electrical machines.